THE ANNALS OF "DUNAREA DE JOS" UNIVERSITY OF GALATI
FASCICLE XI – SHIPBUILDING. ISSN 1221-4620, e-ISSN 2668-3156
2020

IMPACT ANALYSIS TESTS USING FEMAP ADVANCED EXPLICIT DYNAMIC SOLVER

Dumitru-Silviu Perijoc
"Dunarea de Jos" University of Galati,
Faculty of Naval Architecture, Galati,
47 Domneasca Street, 800008, Romania,
E-mail: silviu.perijoc@ugal.ro

Leonard Domnişoru
"Dunarea de Jos" University of Galati,
Faculty of Naval Architecture, Galati,
47 Domneasca Street, 800008, Romania,
E-mail: leonard.domnisoru@ugal.ro

Cristi-Marian Angheluță
"Dunarea de Jos" University of Galati,
Faculty of Naval Architecture, Galati,
47 Domneasca Street, 800008, Romania,
E-mail: marian.angheluta@ugal.ro

ABSTRACT

As part of the continuum growth of the shipping industry, new challenges arise for the engineers. The development of floating structures capable of withstanding accidental loads, such as grounding and ship collisions, become nowadays an integral part of the design process. The current paper presents a methodology for impact analysis using FEMAP software capabilities in two distinct stages. The first stage consists of the impact analysis using a rigid indenter displaced at different speeds. The second stage of the study evaluates the impact analysis considering both the indenter and the structure deformable. Mesh influence tests, as well as the influence of the type of elements used in the analysis, have been taken into consideration in the present study.

Keywords: impact analysis, Femap, material failure, equivalent plastic strain.

1. INTRODUCTION

The advancement in computational power enables a consequent approach of developing large finite element models for marine structures, thus complex phenomena such as ship collision and grounding analysis become manageable [3]. Following the trend of development in computational power, benchmark program suites for structural analysis, such as Siemens Femap [1], introduce in accordance with the demands of the industry, new approaches in numerical analysis and material failure description.

The present study presents a brief insight in the use of Femap [1] for impact structural analysis, considering two types of structures, a simple and stiffened plate. Both structures were subjected to impact, taking into account the indenter as rigid and deformable, traveling at different speeds. (see Table 1)

2. MATERIAL MODEL AND FAILURE CRITERIA

Nonlinear plastic material formulation was used, described by the bilinear stress-strain curve (Fig.1), according to AND [2] material properties formulation for marine graded steel, having the yield stress 235 MPa.

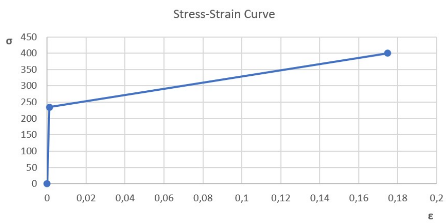

Figure 1. Stress-Strain curve (AND) [2]

Material nonlinearity and rupture failure is controlled by the Advanced Explicit Dynamic Solver (SOL 701) used for solving highly dynamic problems of short duration. The initial von Mises yield criterion was use, having the nonlinear properties isotropic, the hardening rule and the stress-strain curve as the function dependence in Figure 1.

Table 1. Analysed cases

Case	Plate type	Indenter type	v [m/s]	Elem. Size [mm]	μ_c
1	SP	Rigid	2	50	0
2	SP	Rigid	2	50	0,6
3	SP	Rigid	2	25	0
4	SP	Rigid	2	25	0,6
5	SP	Deformable	2	50	0
6	SP	Deformable	2	50	0,6
7	SP	Deformable	2	25	0
8	SP	Deformable	2	25	0,6
9	SP	Rigid	5	50	0
10	SP	Rigid	5	50	0,6
11	SP	Rigid	5	25	0
12	SP	Rigid	5	25	0,6
13	SP	Deformable	5	50	0
14	SP	Deformable	5	50	0,6
15	SP	Deformable	5	25	0
16	SP	Deformable	5	25	0,6
17	ST_PL	Rigid	2	50	0
18	ST_PL	Rigid	2	50	0,6
19	ST_PL	Rigid	2	25	0
20	ST_PL	Rigid	2	25	0,6
21	ST_PL	Deformable	2	50	0
22	ST_PL	Deformable	2	50	0,6
23	ST_PL	Deformable	2	25	0
24	ST_PL	Deformable	2	25	0,6
25	ST_PL	Rigid	5	50	0
26	ST_PL	Rigid	5	50	0,6
27	ST_PL	Rigid	5	25	0
28	ST_PL	Rigid	5	25	0,6
29	ST_PL	Deformable	5	50	0
30	ST_PL	Deformable	5	50	0,6
31	ST_PL	Deformable	5	25	0
32	ST_PL	Deformable	5	25	0,6

3. GEOMETRY AND FEM MODEL

The geometry model consists of a 4000x4000x10 mm plate. The indenter geometry was represented by a semi-sphere object with a diameter of 1000 mm. For the case including the deformable indenter, same dimension of the semi-sphere was considered and two stiffeners plates were added. A thickness of 10 mm was considered for the deformable indenter shell and stiffeners. (Figure 2,3). For the second impacted structure, two 350x10 mm stiffeners were added. (Figure 4,5)

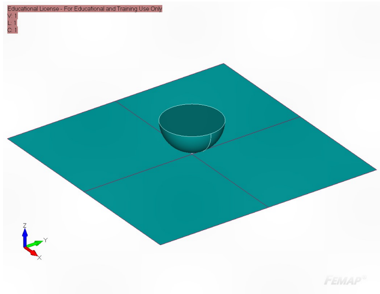

Figure 2. Simple plate – Rigid indenter

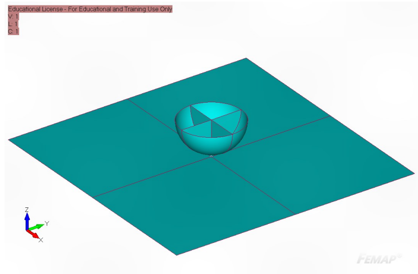

Figure 3. Simple plate – Deformable indenter

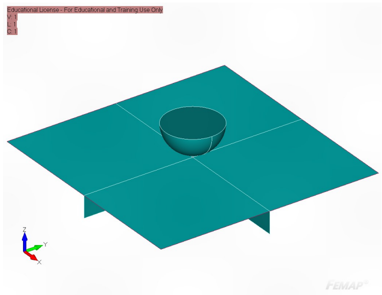

Figure 4. Stiffened plate – Rigid indenter

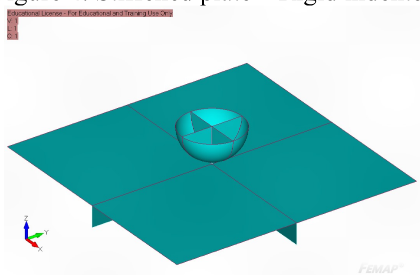

Figure 5. Stiffened plate – Deformable indenter

For the finite element models, the mesh size dimensions of 50 mm and 25 mm are considered, as well as a value of the friction coefficient of μ=0.6. A total of 32 analysis cases are included in the study.

4. Results and discussions

For the impacted simple plate with the rigid and deformable indenter and the velocity of 2 m/s (case 1-8), the next results are obtained:
-Table 2 presents the total contact force variation for rigid and deformable indenters, 50-25 mm mesh size and a friction coefficient value of 0-0.6;
-Table 3 presents the von Mises stress of the impacted plate with the rigid and deformable indenter;
-Figures 6-8 present the resulting von Mises stress resulted following the rigid and deformable indenter impact.

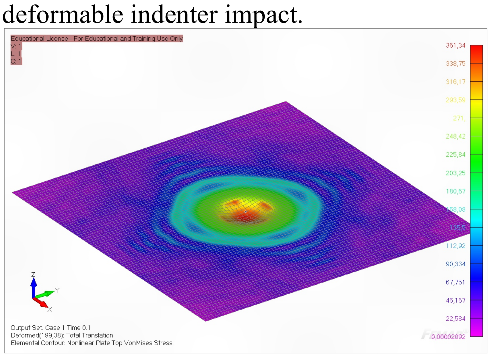

Figure 6. Case 2 – Plate - von Mises stress

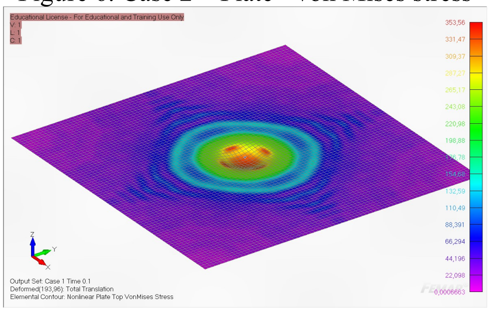

Figure 7. Case 5 – Plate - von Mises stress

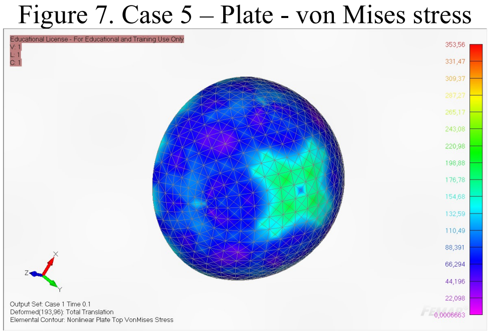

Figure 8. Case 5 – Indenter - von Mises stress

Table 2. Total contact force – 2m/s

Case	Indenter type	Elem. Size [mm]	μ	Total Contact Force [MN]
1	Rigid	50	0	2,030
2	Rigid	50	0,6	2,030
3	Rigid	25	0	1,312
4	Rigid	25	0,6	1,312
5	Deform.	50	0	1,251
6	Deform.	50	0,6	1,251
7	Deform.	25	0	1,035
8	Deform.	25	0,6	1,035

Table 3. von Mises stress – 2m/s

Case	Indenter type	Elem. Size [mm]	μ	σ_{VM} [Mpa]
1	Rigid	50	0	367,07
2	Rigid	50	0,6	361,34
3	Rigid	25	0	371,92
4	Rigid	25	0,6	354,06
5	Deform.	50	0	353,56
6	Deform.	50	0,6	343,57
7	Deform.	25	0	354,79
8	Deform.	25	0,6	351,32

The obtained results for cases 9-16, corresponding to the 5 m/s velocity of the indenter, are described in the following:
-Table 4 presents the total contact force variation for rigid and deformable indenter;
-Table 5 presents the damage volume ratio dependent of the indenter type, mesh dimension and frictional coefficient;

Table 4. Total contact force – 5m/s

Case	Indenter type	Elem. Size [mm]	μ	Total Contact Force [MN]
9	Rigid	50	0	5,020
10	Rigid	50	0,6	5,020
11	Rigid	25	0	3,211
12	Rigid	25	0,6	3,211
13	Deform.	50	0	3,075
14	Deform.	50	0,6	3,074
15	Deform.	25	0	2,914
16	Deform.	25	0,6	2,913

-Figures 9,10 and 11 present the total deformation and von Mises stress distribution of the plate and indenter for the deformable case. The rigid indenter cases point out a clean structural failure of the plate with very small out of plane rotations of the elements.

Table 5. Damage volume ratio – 5 m/s

Case	Indenter type	Elem. Size [mm]	μ	Damage volume ratio
9	Rigid	50	0	4,13%
10	Rigid	50	0,6	4,13%
11	Rigid	25	0	4,86%
12	Rigid	25	0,6	4,57%
13	Deform.	50	0	2,23%
14	Deform.	50	0,6	2,22%
15	Deform.	25	0	3,34%
16	Deform.	25	0,6	2,71%

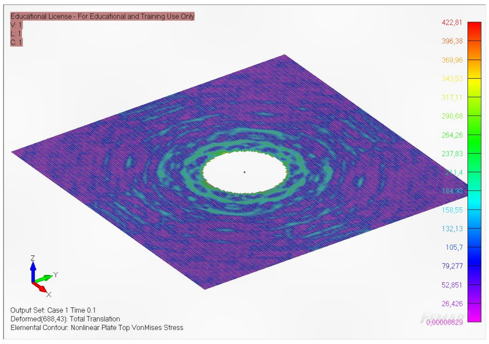

Figure 9. Case 12 - Rigid indenter impact

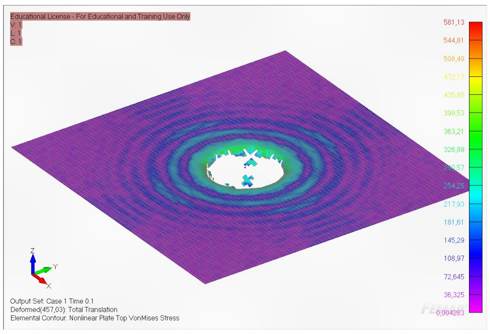

Figure 10. Case 16 - Deformable indenter impact

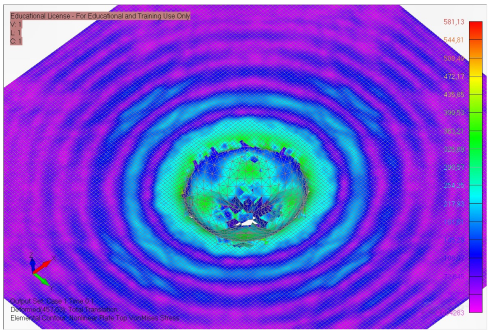

Figure 11. Case 16 - Deformable indenter

For analysed cases 17-24, and the indenter speed of 2 m/s, the following results are obtained:

-Table 6 presents the total contact force resulting after impact.

-Table 7 includes the damage volume ratio resulted after structural failure.

-Figure 12,13,14 presents the von Mises stress distribution and the total deformation occurred on the stiffened panel, as well as on the deformable indenter.

The rigid impact cases register higher values for von Mises stress distribution around the indenter contact area. The combinations of deformations affecting the indenters shape due to impact lead to an overall increase in the stress distribution on the stiffened plate. Structural failure (rupture) was identified for cases 17-20, considering the rigid indenter. Mesh sensitivity can be observed for cases 21-24, corresponding to the deformable indenter, where for the mesh size of 50 mm no element failure was present.

Table 6. Total contact force – 2 m/s

Case	Indenter type	Elem. Size [mm]	μ	Total Contact Force [MN]
17	Rigid	50	0	2,827
18	Rigid	50	0,6	2,827
19	Rigid	25	0	1,756
20	Rigid	25	0,6	1,755
21	Deform.	50	0	1,536
22	Deform.	50	0,6	1,536
23	Deform.	25	0	1,356
24	Deform.	25	0,6	1,357

Table 7. Damage volume ratio – 2 m/s

Case	Indenter type	Elem. Size [mm]	μ	Damage volume ratio
17	Rigid	50	0	0,13%
18	Rigid	50	0,6	0,04%
19	Rigid	25	0	0,43%
20	Rigid	25	0,6	0,45%
21	Deform.	50	0	-
22	Deform.	50	0,6	-
23	Deform.	25	0	0,28%
24	Deform.	25	0,6	0,28%

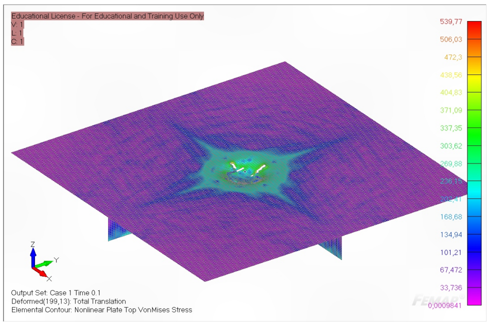

Figure 12. Case 20 - Rigid indenter – 2 m/s

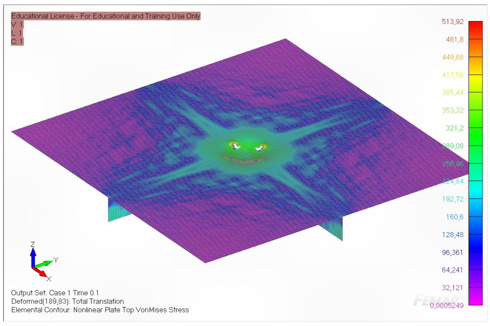

Figure 13. Case 24 - Deformable indenter – 2 m/s

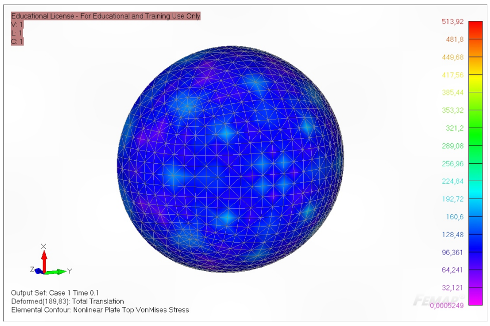

Figure 14. Case 24 - Deformable indenter – 2 m/s

Results for cases 25-32 and indenters velocity of 5 m/s, are presented in the following section:

-Table 8 presents the total contact force.

-Table 9 presents the damage volume ratio.

-Figure 15 presents the von Mises stress distribution and the total deformation of the eroded stiffened panel due to rigid impact.

-Figure 16 presents the von Mises stress distribution following the impact of the stiffened plate with the deformable indenter.

-Figure 17 presents the von Mises stress distribution and deformation for the structure of the indenter.

For the impact cases considering the deformable indenter, out of plane element deformations occurred for both the stiffened plate structure, as well as for the structure of the indenter.

Table 8. Total contact force – 5 m/s

Case	Indenter type	Elem. Size [mm]	μ	Total Contact Force [MN]
25	Rigid	50	0	6,839
26	Rigid	50	0,6	6,839
27	Rigid	25	0	4,353
28	Rigid	25	0,6	4,353
29	Deform.	50	0	6,939
30	Deform.	50	0,6	6,939
31	Deform.	25	0	4,212
32	Deform.	25	0,6	4,212

Table 9. Damage volume ratio – 5 m/s

Case	Indenter type	Elem. Size [mm]	μ	Damage volume ratio
25	Rigid	50	0	4,69%
26	Rigid	50	0,6	4,36%
27	Rigid	25	0	4,40%
28	Rigid	25	0,6	4,28%
29	Deform.	50	0	2,98%
30	Deform.	50	0,6	2,78%
31	Deform.	25	0	3,52%
32	Deform.	25	0,6	2,77%

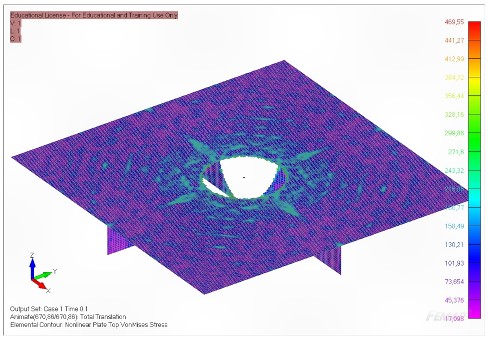

Figure 15. Case 28 - Rigid indenter impact – 5 m/s

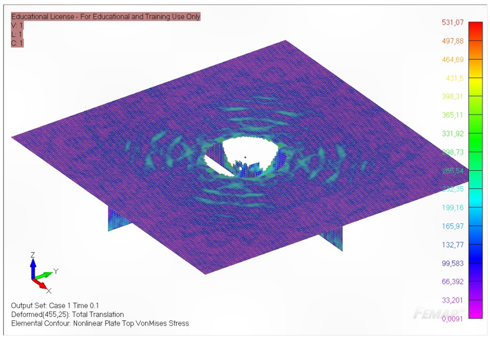

Figure 16. Case 32 - Deformable indenter impact – 5 m/s

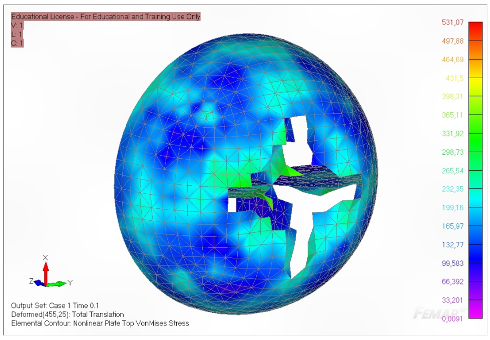

Figure 17. Case 32 - Deformable indenter impact – 5 m/s

5. CONCLUSIONS

The current study presents a brief overview for impact analysis using Femap Advanced Explicit Dynamic solver. The Equivalent von Mises Plastic Strain failure criteria (ε_r=0.1748, σ_r=400 MPa) was used for evaluating structural rupture (AND [2]), taking into consideration the cases of rigid and deformable indenter.

The conclusions following the 32 analysed cases are presented below:

1. Significant differences were obtained for impact analysis considering the indenter rigid or deformable. The damage ratio volume resulted in a smaller value for the cases with deformable indenter.
2. Mesh sensitivity was found to be of great importance in performing the analyses, with significant influence on total contact force and also on the damage volume ratio.
3. The frictional coefficient of 0.6 used in the performed analyses introduced small variation of the damage volume ratio (0.1-0.75%).
4. The total contact force variation was found to be dependent on the mesh size. As the mesh density increased, the local stiffness of the model decreased, resulting in a lower total contact force.
5. Further comparison studies between numerical and experimental data have to be performed in order to validate the numerical solutions.

Acknowledgements

This study is developed in the framework of the Naval Architecture Research Centre, "Dunarea de Jos" University of Galati.

REFERENCES

[1]. **FNN,** *"Femap/NX Nastran users' manual",* Siemens PLM Software Inc., 2020.

[2]. AND, European agreement concerning the international carriage of dangerous goods by inland waterways (Vol. I), 2019. https://doi.org/10.18356/91419305-en

[3]. **ISSC,** "Proceeding of the 20th ISSC Congress", IOS Press, Amsterdam, 2018.

Paper received on October 31^th^, 2020

